Nitrogen Vacancy as the Donor: Experimental Evidence in the Ammonia-Assisted Molecular Beam Epitaxy of GaN

Z. Yang, L. K. Li, J. Alperin, and W. I. Wang*

Department of Electrical Engineering, Columbia University, New York, New York 10027, USA

ABSTRACT

The electron density of unintentionally doped GaN can be reduced by four orders of magnitude by increasing the ammonia (NH_3) beam flux during molecular beam epitaxial growth, indicating that nitrogen vacancies are the donors. This is further evidenced by secondary ion mass spectroscopy measurements on the GaN films which revealed that the concentration of Si residual impurities (the major background unintentional impurity in GaN grown by metallorganic chemical vapor deposition) is far below the carrier concentration and therefore cannot be responsible for the observed background n-type carrier density. With optimized growth parameters, stoichiometric GaN with excellent electrical and photoluminescence properties has been achieved.

Introduction

During the past few years, the qualities of the single-crystal GaN and the related materials have been greatly improved. The GaN-based devices, such as blue light emitting diodes (LEDs),[1] blue laser diodes,[2] and high-temperature/high-power transistors[3,4] have been reported. Although the material properties of GaN have been studied for quite some time, it is still under debate[5-7] whether nitrogen vacancies are donors in GaN films. In this paper, we present evidence to support that nitrogen vacancies are the unintentional donors in GaN films.

Nitrogen vacancies are easily generated in GaN due to the high equilibrium partial pressure of the nitrogen (N_2) in GaN and its wide bandgap energy. The equilibrium nitrogen (N_2) partial pressure of the GaN is 0.07 bar at 800°C [typical molecular beam epitaxy (MBE) growth temperature[8]] and 20 bar at 1000°C [typical metallorganic chemical vapor deposition (MOCVD) growth temperature[9]]. Generally, the growth environments of MBE and MOCVD do not satisfy the required conditions for N_2 equilibrium partial pressure; thus, strict control of the dynamic growth processes is required to suppress nitrogen vacancy formation and obtain device-quality GaN films. With the objective of supplying enough nitrogen for high-quality GaN growth, different nitrogen sources, such as NH_3,[10] electron cyclotron resonance (ECR), and radio frequency (RF) nitrogen plasma[11,12] have been investigated in MBE growth. If the amount of nitrogen is less than required, it is highly probable that nitrogen vacancies will be generated. Nitrogen vacancies can also be introduced by the self-compensation effect of GaN, because the formation energy of a nitrogen vacancy is less than the bandgap energy of GaN.[5,13]

When nitrogen vacancies are formed in GaN, they result in dangling bonds of the surrounding Ga atoms (Fig. 1). These perturbed dangling bond states are the nitrogen vacancy states. In a simplified physical picture, the dangling bond energy can be described by the linear combination of atomic orbital (LCAO) picture, as shown in Fig. 2. In this picture, the outermost orbital of Ga and N atoms linearly combine to form their sp-hybrids separately with energy E_{Ga} and E_N. These two kinds of hybrid orbitals form the Ga-N bonding state at energy E_b and the antibonding state at E_a. The bonding state evolves to the valence band, and the antibonding state evolves to the conduction band of the GaN. Since the Ga dangling bond energy level in GaN derives from the energy level of Ga hybrids, E_{Ga}, the nitrogen vacancy level corresponds to E_{Ga} and acts as a donor. Figure 2 represents the overall physical picture. In order to investigate the electrical properties of the nitrogen vacancy in GaN, we have grown GaN films by ammonia (NH_3)-assisted MBE. The electron density of the unintentionally doped GaN can be reduced by four orders of magnitude simply by increasing the ammonia beam flux during MBE growth, indicating that nitrogen vacancies are the donors. This is further evidenced by the SIMS measurements on the unintentionally doped GaN films, which revealed that the concentration of Si residual impurities is far below the carrier concentration and therefore cannot be responsible for the high-background n-type carrier density in our GaN films.

Experimental

The MBE growth was conducted using a conventional MBE system. A commercial ECR source, an ammonia gas feeding line, and the effusion cells of Ga, Al, In, and Mg were installed in the growth chamber. During the GaN growth at high temperature, NH_3 was fed through a purifier into the growth chamber at a background pressure of 10^{-6} Torr. The flow rate of the NH_3 gas was controlled by a mass flow controller in the range 0 to 200 sccm. GaN growth rate was set at 0.5 μm/h by adjusting the temperature of the Ga effusion cell. The thickness of the GaN

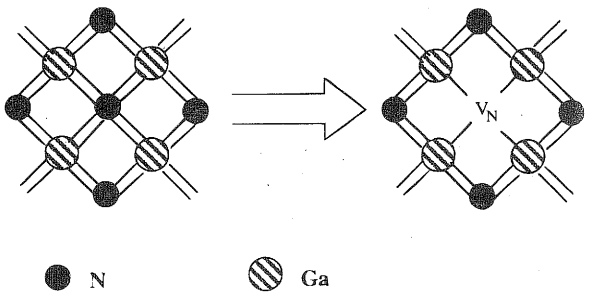

Fig. 1. Schematic atomic geometry of GaN and nitrogen vacancy.

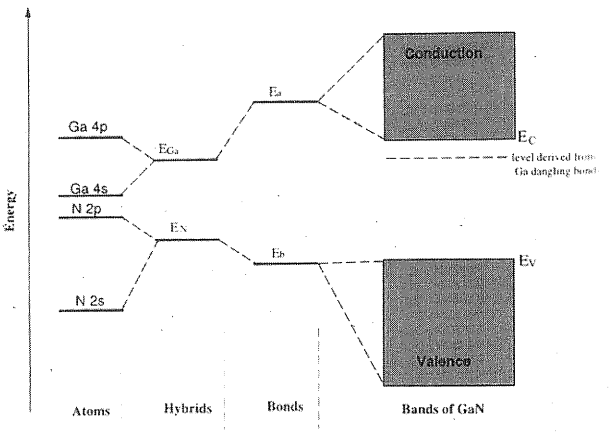

Fig. 2. Schematic LCAO picture of GaN bonds and bands (not drawn to scale).

* Electrochemical Society Active Member.

films was measured by the optical interference spectra in a Fourier transform infrared spectroscope (FTIR). All samples were grown on c-plane sapphire substrates. Before the growth, the sapphire substrates were pretreated by exposing them to the ECR nitrogen plasma at 800°C for 30 min. A 30 nm AlN buffer layer was grown at 550°C. The substrate temperature was raised to 800°C for the subsequent growth of GaN layers. The detailed MBE growth process has been reported elsewhere.[8,10]

Results and Discussion

Background donors can be most thoroughly studied in unintentionally doped GaN films. In our experiments, unintentionally doped GaN films were grown under the same growth rate but with different NH_3 beam flux. The carrier concentration was measured by the van der Pauw-Hall measurement. All the GaN films show n-type conductivity with a wide range of carrier concentrations. Our results clearly showed that lowering the NH_3 flow rate during growth resulted in higher carrier concentration, as shown in Fig. 3. Since lowering the NH_3 flow rate will inevitably result in a higher density of nitrogen vacancies, the high background carrier concentration clearly comes from a high concentration of the nitrogen vacancies. Thus, nitrogen vacancies are donors in GaN and responsible for the n-type conductivity. With the NH_3 flow rate of less than 5 sccm, the GaN films exhibited a large background carrier density (more than 10^{20} cm^{-3}) because the films were nonstoichiometric. The GaN films also showed very weak photoluminescence emission. As the NH_3 flow rate increased, both the electrical and optical properties of the GaN films were improved. With more than 30 sccm ammonia, the background carrier concentration decreased to 10^{16} cm^{-3}. p-Type GaN films can be achieved at the same growth conditions by adding the Mg dopant.[8,13] The improvement of optical properties with increasing NH_3 flow rate is apparent, as shown in Fig. 4.

Instead of nitrogen vacancies, background impurity of Si and oxygen are also responsible for the n-type conductivity of unintentionally doped GaN.[9] The ultrahigh vacuum growth environment of the MBE system ensures that only a small amount of residual Si and oxygen exists in the growth environment. After the thoroughly high-temperature degassing of the MBE sources (main sources of oxygen), the oxygen density in our MBE GaN can be reduced to the lower range of 10^{16} cm^{-3} and cannot be detected by secondary ion mass spectroscopy (SIMS). The background Si in our MBE system could come from the NH_3 gas. It is well known that Si is the major background unintentional impurity in GaN grown by MOCVD.[14] To investigate the role of the background Si in our GaN films, SIMS depth profile measurements were performed on the films. As show in Fig. 5, the Si atom concentration in our GaN film is approximately 5×10^{16} cm^{-3}, much less than the n-type carrier concentration (9.3×10^{18} cm^{-3}) of the sample. Therefore, the background Si impurities cannot account for the background donors in our MBE GaN samples. This SIMS result further evidenced that nitrogen vacancies are the donors in GaN films and are responsible for n-type conductivity of the unintentionally doped GaN. Our observations are consistent with the results of Tansley and Egan which indicate that nitrogen vacancies are donors and their energy level is 400 meV below the GaN conduction band.[6]

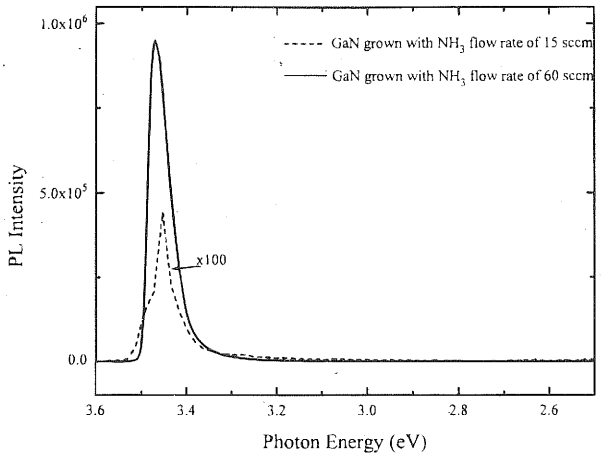

Fig. 4. 10 K photoluminescence spectra of GaN grown with different ammonia flow rates.

Conclusion

The results from Hall and SIMS measurements on unintentionally doped GaN grown by ammonia-assisted MBE indicate that nitrogen vacancies are the donors in GaN. Given insufficient nitrogen during the GaN growth, the resulting nitrogen vacancies can be the dominant background donors. Careful control of the growth parameters is required to obtain high-quality GaN films.

Acknowledgment

This work was supported by DARPA and the Office of Naval Research.

Manuscript submitted March 17, 1997; revised manuscript received June 2, 1997.

Columbia University assisted in meeting the publication costs of this article.

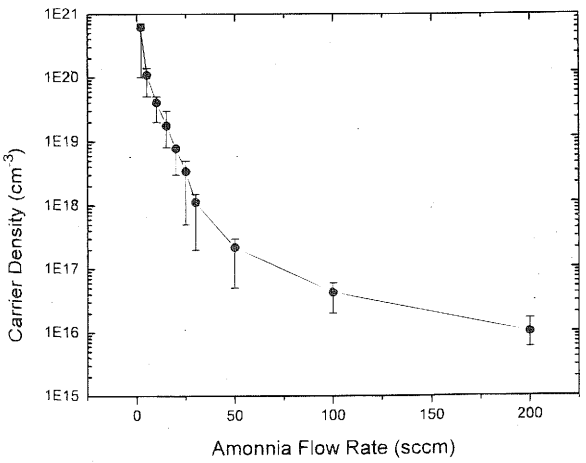

Fig. 3. Electron density of unintentional doped GaN *vs.* ammonia flow rate employed in the NH_3-assisted MBE growth.

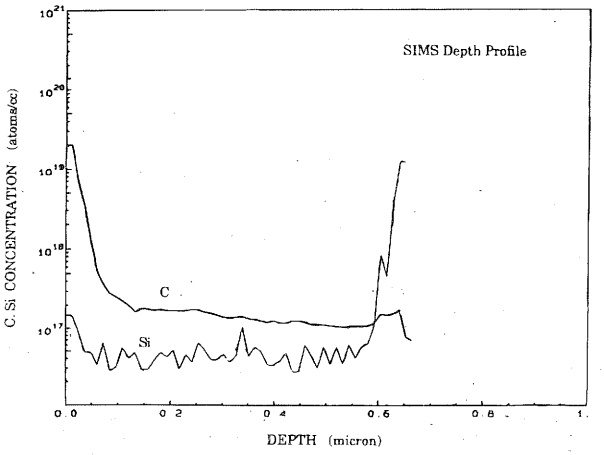

Fig. 5. SIMS depth profile of undoped GaN with background electron density 9.3×10^{18} cm^{-3}.

REFERENCES

1. S. Nakamura, *SPIE-Int. Soc. Opt. Eng.*, **2693**, 43 (1996).
2. S. Nakamura, S. M. Senoh, S. Nagahama, N. Iwasa, T. Yamada, T. Matsushita, Y. Sugimoto, and H. Kiyoku, *Appl. Phys. Lett.*, **69**, 4056 (1996).
3. J. Burm, K. Chu, W. A. Davis, W. J. Schaff, L. F. Eastman, and T. J. Eustis, *ibid.*, **70**, 464 (1997).
4. J. Pankove, S. S. Chang, H. C. Lee, R. J. Molnar, T. D. Moustakas, and B. Van Zeghbroeck, *Tech. Dig. Int. Electron Devices Meet.*, (Cat. No.94CH35706), 947 (1994).
5. J. I. Pankove, *Mater. Res. Soc. Symp. Proc.*, **162**, 515 (1990).
6. T. L. Tansley and R. J. Egan, *Phys. Rev.*, **B45**, 10942 (1992).
7. J. Neugebauer and C. G. van de Walle, *ibid.*, **B50**, 8067 (1994).
8. Z. Yang, L. K. Li, and W. I. Wang, *Appl. Phys. Lett.*, **67**, 1686 (1995).
9. I. Akasaki and H. Amano, *This Journal.*, **141**, 2266 (1994).
10. L. K. Li, Z. Yang, and W. I. Wang, *Electron. Lett.*, **31**, 2127 (1995).
11. R. J. Molnar and T. D. Moustakas, *J. Appl. Phys.*, **76**, 4587 (1994).
12. Z. Yang, F. Guarin, I. W. Tao, W. I. Wang, and S. S. Iyer, *J. Vac. Sci. Technol.*, **B13**, 789 (1995).
13. Z. Yang, L. K. Li, and W. I. Wang, *Mater. Res. Soc. Symp. Proc.*, **395**, 169 (1996).
14. J. Neugebauer, and C. G. van de Walle, in *22nd International Conference on the Physics of Semiconductors*, D. J. Lockwood, Editor, Vol. 3, pp. 2327-2330, ICPS, Vancouver,. BC, Canada (1994).

Revised Pourbaix Diagrams for Copper at 25 to 300°C

B. Beverskog[a] and I. Puigdomenech[b]

Studsvik Material AB, S-611 82 Nyköping, Sweden

ABSTRACT

The Pourbaix diagrams (potential-pH diagrams) for copper at 25 to 300°C have been revised. Extrapolation of thermochemical data to elevated temperatures has been performed with the revised model of Helgeson-Kirkham-Flowers, which also allows uncharged aqueous complexes, such as CuOH(aq) and $Cu(OH)_2$(aq), to be handled. Calculated high temperature thermodynamic data have been fitted against experimental data at elevated temperature. The hydrolysis of copper(I) and (II) is included with two and four hydroxide complexes, respectively. The Pourbaix diagrams show that the oxides (Cu_2O(cr) and CuO(cr)) are stable at 25 to 200°C at 10^{-6} mol kg^{-1} of dissolved species, and at 300°C only CuO is stable. The oxides are stable at 25°C at 10^{-8} mol kg^{-1}, but at 100 to 300°C no solid compound is stable.

Introduction

The corrosion properties of the chemical system copper-water have been studied from a thermodynamic point of view in a number of instances. The choice of aqueous copper species is very similar in all these publications. However, there has been a substantial progress lately in chemical analysis of aqueous copper species, and the aqueous complexes of copper in previously published works are not always in agreement with modern conceptions of these species. This motivates a reconsideration of the thermodynamic fundamentals for the corrosion properties of the aqueous copper system.

Pourbaix diagrams for copper can be found in a large number of publications, but studies which include calculations to create Pourbaix diagrams are relatively few.[1-13] At temperatures above 25°C there are only four published Pourbaix diagrams for copper.[4,8,9,12]

The aim of this work was to revise the Pourbaix diagram for copper at elevated temperatures and to calculate temperature effects below 25°C, which have not been published before. This report is the first of a series of studies where sulfur, chlorine, and carbon are intended to be included in the study of the corrosion properties of copper.

Pourbaix diagrams are suitably complemented by predominance diagrams for dissolved aqueous species in the system. This type of chemical equilibrium diagram contains only dissolved species and is used to determine the predominance of aqueous ions and complexes where a solid phase is thermodynamically stable and hides the aqueous species in the corresponding Pourbaix diagram.

Choice of Copper Species

It is of basic importance which species (solid phases, fluids, aqua ions, and aqua complexes) are included in the thermodynamic calculations in a given chemical system. Some species are not stable in water solutions while others can only form at high temperatures or at extreme compositions. It is therefore of the greatest importance to critically evaluate the species which are expected to exist in a system before they are allowed to be the basis for the thermodynamic calculations. Calculations based on wrong species give misleading information of chemical equilibria.

Copper has the electron configuration $[Ar]3d^{10}4s^1$, *i.e.*, one lone 4s-electron outside full 3d-orbitals. As a consequence, the first ionization enthalpy is high compared with other elements with the oxidation number +I like the alkali metals. The ionization enthalpies for the second and the third oxidation step for copper are much lower than those for the alkali metals and this partly contributes to its character of transition metal. The oxidation numbers for copper in aqueous solution are 0, I, and II. Trivalent copper is a very strong oxidizing agent and thereby not stable in water.

The choice of copper species, which is the basis for the construction of Pourbaix diagrams, has been made in a very traditional and routine manner in earlier publications, see Table I. Mostly it has been the same set as in the thesis of Pourbaix in 1945. There is an agreement on three solid phases: Cu(cr), Cu_2O(cr), and CuO(cr). The hydroxide is included in six publications. Of the dissolved species, only Cu^+, Cu^{2+}, and $HCuO_2^-$ and/or CuO_2^{2-} were included in the majority of cases. The first and second hydrolysis steps for Cu(I) and Cu(II), respectively, have not been included in previous publications. The nomenclature $Cu(OH)_n^{2-n}$ for the third and fourth hydrolysis steps for Cu(II) has been used in only one study.[13] A polynuclear hydrolysis species was included in Ref. 7. Copper(III) species were included in Ref. 5, 7, and 10.

Ten dissolved species and four solid compounds have been selected as the ground for the revised thermodynamic calculations in the copper-water system accounted here, see Table II.

The justifications for excluding species are as follows: the copper(I) hydroxide is not stable in aqueous solutions.[6]

[a] Present address: Institutt for energiteknikk, OECD Halden Reactor Project, N-17 77 Halden, Norway.
[b] Present address: Department of Inorganic Chemistry, Royal Institute of Technology, S-100 44 Stockholm, Sweden.